Novel plasma source for safe beryllium spectral line studies in the presence of beryllium dust

B. D. Stankov, M. Vinić, M. R. Gavrilović Božović, and M. Ivković

Citation: Review of Scientific Instruments **89**, 053108 (2018); doi: 10.1063/1.5025890
View online: https://doi.org/10.1063/1.5025890
View Table of Contents: http://aip.scitation.org/toc/rsi/89/5
Published by the American Institute of Physics

Novel plasma source for safe beryllium spectral line studies in the presence of beryllium dust

B. D. Stankov,[1,2] M. Vinić,[1] M. R. Gavrilović Božović,[1] and M. Ivković[1,a)]
[1]*Institute of Physics, University of Belgrade, P.O. Box 68, 11080 Belgrade, Serbia*
[2]*Faculty of Sciences, Department of Physics, University of Novi Sad, Trg Dositeja Obradovića 4, 21000 Novi Sad, Serbia*

(Received 14 February 2018; accepted 22 April 2018; published online 11 May 2018)

Plasma source for beryllium spectral line studies in the presence of beryllium dust particles was realised. The guideline during construction was to prevent exposure to formed dust, considering the toxicity of beryllium. Plasma source characterization through determination of optimal working conditions is described. The necessary conditions for Be spectral line appearance and optimal conditions for line shape measurements are found. It is proven experimentally that under these conditions dust appears coincidently with the second current maximum. The electron density measured after discharge current maximum is determined from the peak separation of the hydrogen Balmer beta spectral line, and the electron temperature is determined from the ratios of the relative intensities of Be spectral lines emitted from successive ionized stages of atoms. Maximum values of electron density and temperature are measured to be 9.3×10^{22} m^{-3} and 16 800 K, respectively. Construction details and testing of the BeO discharge tube in comparison with SiO_2 and Al_2O_3 discharge tubes are also presented in this paper. *Published by AIP Publishing.*
https://doi.org/10.1063/1.5025890

I. INTRODUCTION

The interest for Be spectral lines studies stems from the prevalence of Be, which occurs in nature and is used in many devices. Beryllium is an element which has six times the specific stiffness of steel and at the same time it is one-third lighter than aluminum. This unusual combination of properties makes it suitable for a wide range of applications: aerospace, military, information technologies, energy exploration, medical, and other advanced applications. The three most used forms of beryllium are beryllium-containing alloys, pure beryllium metal, and beryllium ceramics, also known as beryllium oxide ceramic.

Since Be is also a naturally occurring element in metal-poor stars,[1] the study of the spectral lines emission of beryllium is important for astrophysics. For example, spectral lines coming from Be II deexcitation at 313.0 nm and 313.1 nm are used for the analysis of some stars' origin.[2] Hence, basic knowledge about beryllium spectral emission is available but still, according to critical reviews,[3–9] spectroscopic investigations and Stark parameters' studies are almost exclusively limited to Be II resonance lines at 313 nm.[10–13] In several of these studies,[10–12] the plasma source was an electromagnetically driven "T" tube. Beryllium was deposited in the form of thin layers of $BeCl_2$ on the electrode[10,11,13] and by dusting the quartz tube with $BeCl_2$.[12]

Because of its low atomic number and very low absorption for X-rays, the oldest and still one of the most important applications of beryllium is in radiation windows for X-ray tubes.[14,15]

Also, the beryllium has been chosen as the element to cover the first wall of ITER (International Thermonuclear Experimental Reactor). The first wall of ITER is a part of the blanket that is constructed with 440 panels that completely cover inner wall of the vacuum vessel. Those panels will be covered with 8-10 mm of beryllium armor, leading to approximately 12 tons of beryllium in total, distributed over a surface area of about 700 m^2 (Ref. 16, Sec. 13.3.1.2). In addition, beryllium oxide is also used as insulation in some ITER components (Ref. 16, Table 13.3-1). Beryllium is the material of choice in ITER due to its light weight, low tritium absorption, and efficient trapping of oxygen impurities at its surface forming BeO. The drawback of Be is its low melting temperature what makes it vulnerable to edge-localized modes (ELMs) and disruptions.[17] ELMs and disruptions may provoke large thermal transient loads on beryllium components of the first wall leading to rapid heating of the beryllium surface. Rapid heating can result in plasma-surface interaction processes and can lead to material loss, melting, evaporation, and formation of beryllium dust. Erosion of beryllium under transient plasma loads will determine a lifetime of ITER first wall.[18] The presence of dust particles in fusion reactors has several consequences. There is a safety issue because Be is toxic in the case of inhalation, so constant air monitoring must be provided.[19] Other problems regard the pollution of the plasma by particles, causing the reduced performance, or its deposition on diagnostic equipment. Still, the knowledge of dust creation processes and behavior in a plasma environment is very limited,[20] partially due to the previously mentioned safety issues when handling plasma sources with toxic materials, as beryllium.

Research on dusty plasma is gaining in popularity due to its unique properties and importance for novel technologies.[21] Furthermore, the dust in plasma shows interesting

a)Author to whom correspondence should be addressed: milivoje.ivkovic@ipb.ac.rs

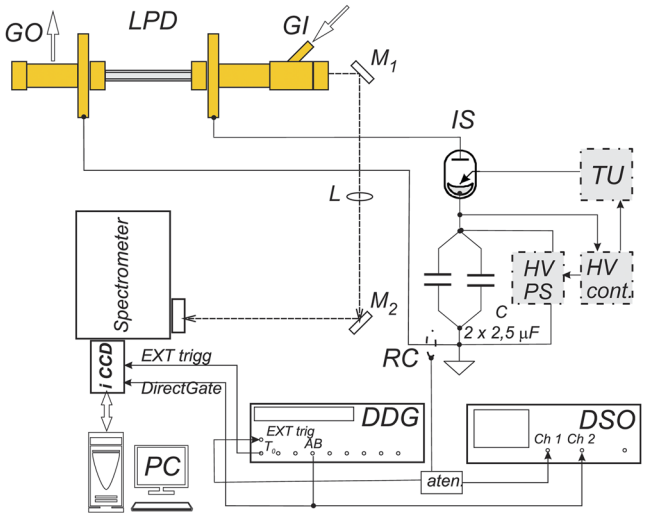

FIG. 1. Experimental setup, LPD—linear pulsed discharge, GO—gas outlet, GI—gas inlet, M_1—mirror, L—lens, M_2—mirror, IS—ignitron switch, TU—trigger unit, HV PS—high voltage power supply, RC—Rogowski coil, DSO—digital storage oscilloscope, DDG—digital delay generator, ICCD—Intensified Charge Coupled Device camera, PC—personal computer.

fundamental phenomena like plasma crystals and dust acoustic waves.[22–24] In many applications, besides already mentioned ITER, the dust in plasma is the unwanted effect, e.g., for plasma etching and thin film deposition in semiconductor industry. This increases the relevance of dust particle formation studies and sets the need to relate it to some other physical phenomenon, like spectral emission from the tokamak plasma.[25,26]

In addition, *in situ* examination of plasma facing materials in tokamak (beryllium and others) by laser induced breakdown spectroscopy (LIBS)[27,28] requires the knowledge of their atomic data (transition probabilities, Stark broadening parameters, etc.). The lack of Stark parameters for Be spectral lines was one of the main inspirations for this plasma source construction.

The main goal of this work was not only to obtain a stable plasma source for the beryllium spectral lines' study but also to enable the examination of dust particles' influence on emission spectra when optimal conditions for Be spectral emission are achieved. The idea was to obtain beryllium spectral lines from erosion of the beryllium oxide, BeO discharge tube, and preferentially, the lines belonging to transitions other than resonant, which are the only ones studied in detail up to now. To draw an analogy with previous studies[10–13] in the experiemental setup we used, beryllium was introduced through the ablation of a ceramic tube settled inside the discharge tube, which allowed more consistent ablation, longer and more reliable work, and appearance of various Be spectral lines. In order to closer investigate the influence of specific discharge tube material on dust particle production and emission spectra, two additional discharge tubes were made. Construction details and testing of the BeO discharge tube in comparison with SiO_2 and Al_2O_3 discharge tubes are also presented in this paper.

II. EXPERIMENT

The experimental setup is presented in Fig. 1. Capacitor C is charged between 4 and 8 kV, using a high voltage power supply, HV PS, operated through the laboratory made high voltage control. When voltage reaches a selected value, the pulse is generated by high voltage control and shaped by the trigger unit in order to initiate ignitron switch, which starts the current flow through the linear pulsed discharge tube. The current shape is monitored by the Rogowski coil and recorded with a digital storage oscilloscope, DSO (Tektronix TDS 360); see typical current shapes for different discharge tubes in Fig. 2(a). The same but attenuated signal from the Rogowski coil is used for the triggering of intensified charge coupled device (ICCD) camera (Andor DH720); see Fig. 1. The acquisition gate width, t_G, and delay, t_D, are determined with a Digital Delay Generator (DDG) (Stanford Research Systems SRS, Model DG535). The spectra are recorded using a gate width of 50 ns at different delays in order to determine the temporal evolution of plasma parameters.

The 1:1 image of the radiation emitted end-on along the axis of the discharge tube is projected on the entrance slit (20 μm wide) of the Shamrock 303 (Andor) imaging spectrometer using folding mirrors M_1 and M_2 and a quartz achromatic lens (focal length f = 33 cm). The change of the diffraction grating (300, 1200, or 2400 groves/mm), slit width, and wavelength position is performed using the commercial Andor Solis software. The instrumental width with 2400 g/mm grating and 20 μm slit width determined using Oriel penlight calibration lamps is 0.09 nm.

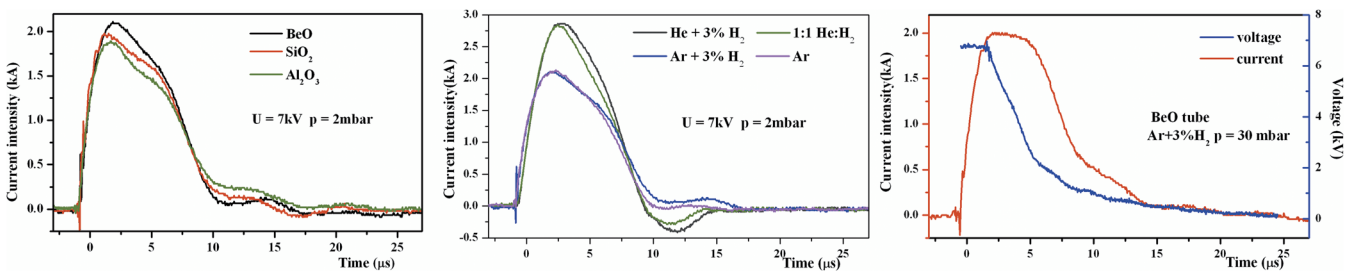

(a) (b) (c)

FIG. 2. Current shapes for (a) different discharge tubes for the same gas type Ar + 3% H_2, pressure p = 2 mbar, and discharge voltage U = 7 kV, (b) BeO tube with different gasses at the same pressure 2 mbar and the same voltage 7 kV, (c) temporal evolution of voltage and current for the BeO tube and Ar + 3% H_2.

III. EXPERIMENTAL DETAILS AND PROCEDURE

The discharge tube was made and studied under different experimental conditions. Electrode material and dimension, electrodes separation, discharge voltage, initial discharge pressure, and direction of various gas flows through the tube, see Fig. 3, were alternated. The general layout and construction details of discharge tubes with special attention on safety measures are given first in Sec. III A, followed by the electrical characterization and optimization of the discharge in Sec. III B. Influence of discharge parameters on emission spectra is fully described and discussed in Sec. III C, while appearance and some properties of the dust particles formed during the discharge operation are described in the Sec. III D.

A. Construction details of the discharge tubes

According to Material Safety Data Sheets, MSDS,[29] beryllium, BeO, and especially their dust are highly toxic and must be handled with great precautions. Therefore, the BeO discharge tube with an inner diameter of 2.6 mm, an outer diameter of 10 mm, and an overall length of 130 mm was settled inside the Pyrex glass tube with an inner diameter of 11.5 mm, an outer diameter of 14 mm, and an overall length of 140 mm; see Fig. 3(a). In such a way, exposure of the beryllium tube to atmosphere was prevented. The position of the inner (ceramic) tube inside the outer (glass) tube was adjusted using Teflon rings or Teflon tape; see Fig. 3(a). This extra space prevented cracking or destruction of the tube due to the significant mismatch in the thermal expansion coefficient between the Pyrex glass and BeO tube and/or destruction caused by shock waves generated by pulsed discharge.

Several additional safety measures were undertaken to prevent exposure to beryllium oxide components and especially to the BeO dust. When handling the BeO tube, the surgical gloves, surgical mask, laboratory coat, and goggles were used. Assembling and manipulation of the discharge tube were performed in the fume hood of the chemical part of the laboratory.

The discharge tube connectors had a gas inlet or outlet port and an electrode holder in the middle, ending with Wilson connectors for vacuum tight connection on one side and quartz windows for spectroscopic observations on the other side; see Fig. 3(b). The position of the high voltage connections and electrically isolated support is also presented in Fig. 3(b). Discharge tubes worked under low pressure continuous gas flow. The gas was supplied from the gas cylinder using the regulation and needle valve, with continuous monitoring of gas pressure on the inlet side of the tube. Two positions of the tube inlet were tested, 90° angle and 45° angle relative to the discharge tube axis. The liquid nitrogen cooled trap and HEPA (high efficiency particulate air) filter were inserted in the front of and at the exit of the rotary vane vacuum pump. Gas exhaust from the vacuum pump lead to the pump settled outside the laboratory and equipped with an additional filter.

Two additional tubes were used for the comparative study of the discharge tube material influence on the dust generation. The first one, made of alumina ceramics, Al_2O_3, with an inner diameter of 2.6 mm, an outer diameter of 10 mm, and an overall length of 125 mm was settled inside the glass tube with the same dimensions as the one used for the BeO tube. The second one, made of quartz, SiO_2, with an inner diameter of 3 mm, an outer diameter of 6 mm, and an overall length of 140 mm was attached with an additional adapter to the same construction; see Fig. 3(c). In Fig. 3(a), the inner diameter of the hollow electrodes, ***d***, is presented. Throughout the experimental course of the study, the value of ***d*** was changing between 0.6 mm and 2 mm.

B. Electrical characterization and optimization

In this study, different gasses (Ar, Ar with 3% of H_2, He + 3% of H_2 and 1:1 He/H_2 mixture) at different pressures (1, 2, 3, 4, 5, 10, 20, and 90 mbar) were used. As the first step, Pashen curves were determined, and then current shapes were recorded for each gas/pressure/voltage combination. Typical examples of voltage and current shapes are presented in Fig. 2. Current shapes for different tube materials at the same conditions are presented in Fig. 2(a). Comparison of current shapes for the BeO tube with different gasses is illustrated in Fig. 2(b). Temporal evolution of voltage and current for the BeO tube are is presented in Fig. 2(c). As can be seen from the current curves in Fig. 2, the duration of the current pulse was around 10 μs, while the current maximum was detected around 3 μs. Besides the basic condition that the discharge voltage must be larger than breakdown voltage, its value should be chosen in a way that parasitic discharge in the space between the ceramic and glass tube, see Fig. 3(a), is avoided. Such discharge may not only introduce spectral lines of impurities in the recorded

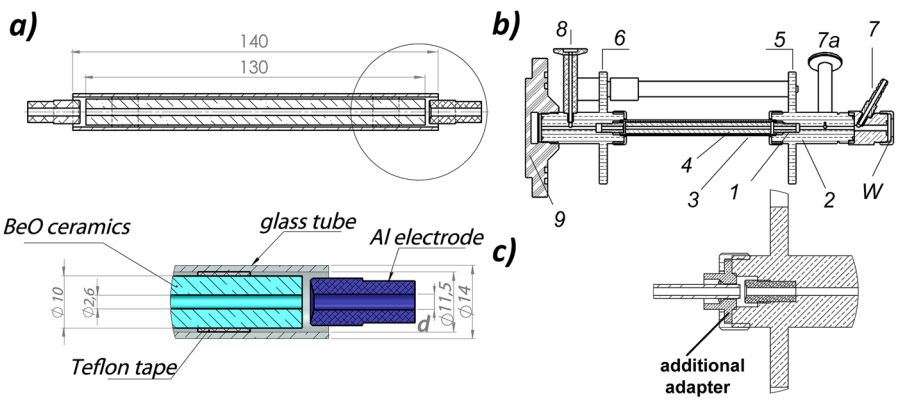

FIG. 3. (a) Construction of the BeO tube and its position inside the glass tube; (b) discharge tube: (1) electrode, (2) holding body, (3) Pyrex glass tube, (4) tube made of BeO or Al_2O_3, (5) anode connection, (6) cathode connection, (7) gas inlet at 45° angle, (7a) gas inlet at 90° angle, (8) gas outlet, (9) dielectric support; (c) additional adapter used for the SiO_2 tube.

spectrum but also burn the Teflon tape and cause total destruction of the discharge light source. In order to prevent this phenomenon, the discharge tube was first constructed in such a way that electrodes come in the ceramic tube; see Fig. 3. Therefore, the part of the electrode that goes inside the ceramic tube must have outer diameter smaller than 2.6 mm, limiting the maximum inner diameter of the electrode to 1.5 mm. Such electrodes also centre the ceramic tube inside the glass tube. However, the parasitic discharge still appears, Sec. III A. In addition, the optical signal from discharge tubes with such electrodes had very low intensity and poor reproducibility. Therefore, further measurements were performed with construction having a small separation between the ceramic tube and electrodes, and with the Teflon rings being placed toward the middle of the discharge tube. In this configuration, parasitic discharge has never appeared.

Three types of electrodes were tested. First, the electrode made of tungsten with an opening of $\boldsymbol{d}$ = 0.6 mm described earlier[30] was used. The idea was to obtain plasma with higher electron densities and additional plasma emission from the plasma jet at the outer side of the electrode, see Ref. 31, in order to use the spectral line emitted from the plasma jet as a reference line for wavelength shift measurements. Unfortunately, spectral lines of beryllium from the jet were not detected, while the radiation intensity was very low, in addition with a poor reproducibility. The spectra recorded using aluminum alloy electrodes with inner diameters 2 and 3 mm showed similar behavior irrespective of the diameter, while the signal to noise ratio was higher with larger electrode openings. Therefore, all further measurements were performed using aluminum alloy electrodes with 3 mm inner diameter. It should be stressed that under used experimental conditions spectral lines of the electrode material (tungsten and aluminum alloy $AlMgCu_5$) were not observed in the case of the BeO and Al_2O_3 tube.

For the optimal conditions for the BeO tube, see Sec. III C 2, the maximum current value goes up to 2.1 kA. The current minimum (observed in the case of He/H_2 mixtures) is caused by the change of plasma impedance resulting in periodic current pulse behavior. Namely, the resistor in the discharge circuit was chosen to obtain the aperiodic current pulse with Ar, which is not optimal for discharge with He. The origin of the second maximum detected only when working with Ar and Ar with 3% H_2, see Fig. 2, is somewhat more complex and it will be addressed later in Sec. III D.

Here, one should notice that for different inner diameters of BeO, Al_2O_3, and SiO_2 tubes, current densities through the discharge tubes are different as well: 98 A/mm^2 for BeO, 87 A/mm^2 for Al_2O_3, and j = 69 A/mm^2 for SiO_2. Taking into account different tube lengths, the energy densities are 0.058 J/mm^2, 0.06 J/mm^2, and 0.046 J/mm^2 for BeO, Al_2O_3, and SiO_2 tubes, respectively.

C. Spectra recordings

Since the main objective of this work was the construction of a safe and stable plasma source for beryllium spectral lines' recording, the next step was to examine the change of the spectra under different discharge conditions. Construction details ($\boldsymbol{d}$, gas flow direction), gas type and gas pressure, discharge voltages, etc. were varied and their influence on recorded spectra was monitored. All spectroscopic studies were performed in three steps. The position of the projected plasma image on the ICCD sensor was checked through the recordings with the fully open slit of the imaging spectrometer and with the grating in the zero diffraction order. Afterwards, overall spectra were recorded with the shortest possible delay from the beginning of the current pulse (800 ns in this experiment, determined by reliable triggering of the ICCD camera) using a gate width of 50 ns. Finally, the temporal evolution of the spectra under various conditions was obtained and the influence of the particular discharge condition was studied. The influence of the different construction geometries on discharge operation has already been addressed in Secs. III A and III B, while here the impact of the gas type, pressure, flow, and different applied voltages on the quality of spectral emission is inspected more closely.

1. Discharge gas

To study the influence of the gas type on spectra recording, i.e., on the appearance of the tube material's spectral lines, three carrier gasses were used, He with 3% H_2, Ar, and Ar with 3% H_2. The 1:1 He/H_2 mixture was excluded from further measurements since beryllium lines were difficult to detect. Helium was chosen as one of the possible solutions for carrier gas because it has a small amount of spectral lines, while hydrogen is added for diagnostic purposes, since it enabled diagnostics of electron density using separation of the hydrogen Balmer beta line-peaks method.[32] At 1 mbar of gas pressure, capacitor C = 5 μF charged to 7 kV, and delay of 12 μs, spectral lines of Be were narrower and had much lower intensity for He + 3% H_2 in comparison to Ar and Ar with 3% H_2; see Fig. 4. With He + 3% H_2 as a carrier gas, only prominent lines of Be appeared in current decay and lasted only few μs. By contrast, with Ar and Ar with 3% H_2, lines of Be lasted 8 μs longer. The highest intensity of Be lines was obtained using the Ar/H_2 mixture. Therefore, all proceeding measurements were conducted using Ar with 3% H_2.

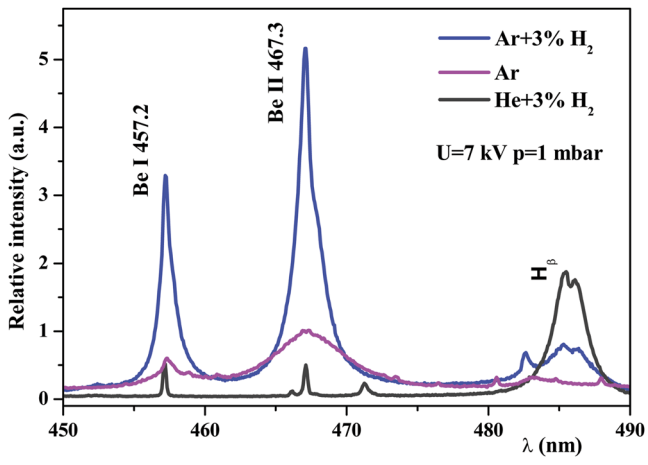

FIG. 4. Influence of different gasses, Ar with 3% H_2, Ar and He with 3% H_2, on spectral line shapes of beryllium lines and the hydrogen Balmer beta, at discharge voltage 7 kV and pressure 1 mbar, delay 12 μs.

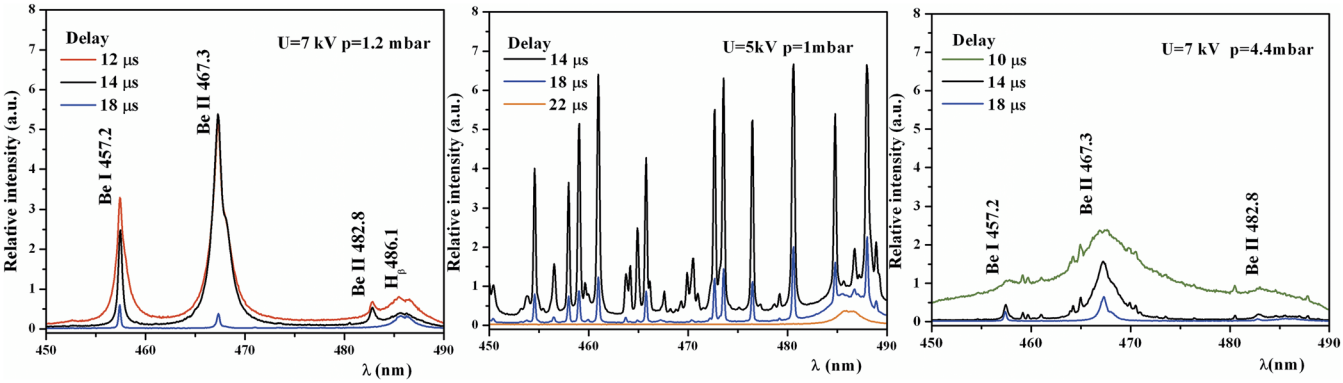

FIG. 5. Influence of different discharge voltage and pressure on spectral line shapes of beryllium in argon with 3% of hydrogen.

Under certain conditions, discussed later in Sec. III D, the dust of the discharge tube material was produced and often accumulated in small electrode openings (if smaller than 2 mm). These particles prevented evacuation of the discharge tube. In addition, with electrodes with 3 mm opening, the dust particles were reaching the observation window, causing degradation of transmittance and lowering of the optical signal. Since the increase of the gas flow rate did not eliminate deposition of dust particles on the observation window, the gas flow direction was reversed; see Fig. 3(b). Also, the additional adapter inlet enabling gas flow under the 45° angle was introduced, see Fig. 3(b), which also helped in preventing dust particle deposition on the window. It was confirmed that the change of the gas flow direction did not affect the spectra recordings, so for the rest of the measurements gas was flowing from the output window toward the discharge tube support.

2. Discharge voltage and gas pressure

Spectra recorded for the same gas, pressure, and gate width but different discharge voltages vary significantly. Namely, the differences between spectra were reflected in line intensity, line width, and in appearance of non-beryllium lines. As can be seen in Fig. 5(a), at 7 kV voltage, the beryllium lines are clearly distinguishable, while Ar lines are not observed at delays greater than 10 μs, i.e., after the current pulse. On the contrary, at a discharge voltage of 5 kV, spectra are rich in spectral lines of discharge gas. Spectral lines of the gas appeared during and lasted after the current pulse, while spectral lines of the tube material were not observed, Fig. 5(b). That is probably due to low abrasion, i.e., low quantity of beryllium in the plasma, or due to overlapping of Be spectral lines with stronger lines of Ar. The same is to be expected when using voltages less than 5 kV. Even though dust particles are produced at voltages of 7 kV, only at higher voltage of 8 kV they were deposited on the glass windows, lowering optical transparency in spite of all undertaken measures described in Sec. III C 1. Therefore, all forthcoming measurements were performed at a discharge voltage of 7 kV.

Gas pressure influences greatly the Be spectral line intensity. A slight increase of pressure leads to more effective excitation of argon and appearance of argon lines in spectra. At a pressure of 4.4 mbar shown in Fig. 5(c), the spectral lines of Be are broader and the continuum is more pronounced, compared to Fig. 5(a). This is most probably due to the increase of electron density. On the other hand, the intensity of Be lines is lower and argon lines are observed. Here, one should have in mind that the spectral line at 467.3 nm presented in Fig. 5 is the most intense beryllium line recorded in this study, i.e., other spectral lines have very low intensity, if observed at all at a pressure of 4.4 mbar and higher. Therefore, all proceeding measurements were conducted at a pressure of 1.2 mbar in order to record spectral lines of beryllium.

The temporal evolution of spectra recorded between 330 nm and 660 nm with the beryllium tube is presented in Fig. 6. The spectra were recorded for the conditions described earlier, i.e., Ar with 3% H_2 and gas pressure 1.2 mbar (gas discharge voltage 7 kV), which were found to be optimal. At early delays (around 10 μs), see Fig. 6, spectral lines of argon and pronounced continuum were evident. After current pulse, the intensity of spectral lines of the discharge tube material was increasing, reaching the maximum value approximately at the time of the second maximum of the current pulse; see Fig. 2. The maximum intensity of the tube material's spectral lines was detected around 12 μs. At that time, lines of Be were prominent and Ar spectral lines were not detected. The beryllium lines were detected in spectra up to 25 μs.

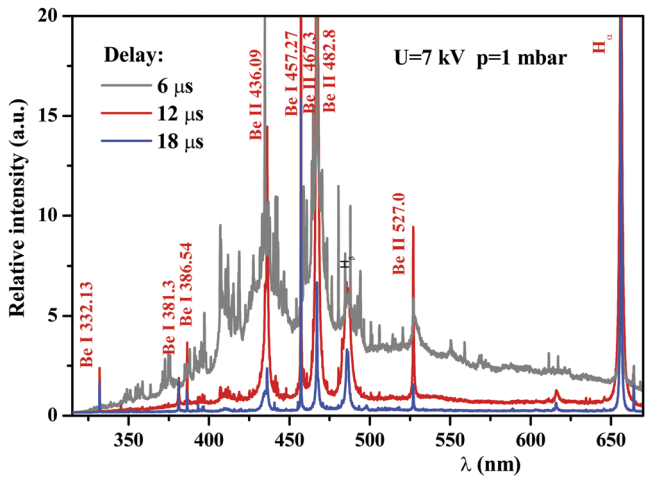

FIG. 6. Temporal evolution of the spectra between 320 nm and 660 nm in low pressure pulsed discharge with the beryllium tube.

3. Comparison of plasma spectrum recorded from different tube materials

As mentioned previously, three different tube materials were used. Emphasis is placed on the BeO tube, while spectra obtained using tubes made from SiO_2 and Al_2O_3 were used for comparison. In Fig. 7, spectra recordings with the tubes made of different materials are presented. The optimal conditions for measuring line shapes of Be were concluded to be at C = 5 μF, U = 7 kV, gas Ar + 3% H_2, and p = 1.2 mbar. At those same conditions, spectral lines of Al emitted from the Al_2O_3 tube were self-reversed, in consequence of self-absorption, while spectra when using the SiO_2 tube could not be recorded because of occasional glass tube breaking and saturation of the optical signal, even with the shortest gate. The best line/continuum ratio for recordings with the glass SiO_2 tube was achieved at C = 5 μF, U = 4 kV, gas Ar + 3% H_2, and p = 3 mbar, while for the Al_2O_3 tube those conditions were at C = 5 μF, U = 6 kV, gas Ar + 3% H_2, and p = 1.5 mbar.

Temporal evolutions of spectral lines emitted from the tube material differ for all the three cases. In early times (during the current pulse), there were no spectral lines of Be or they were not resolved due to overlapping with numerous much stronger Ar lines and intense continuum; see Sec. III C 2. Spectra of lines emitted from the SiO_2 and Al_2O_3 tubes were impossible to record at early delays due to the more intense continuum, which caused saturation of the optical detector even at shortest gate time. As mentioned in Sec. III C 2, the lines of beryllium were detected in spectra up to 25 μs delay. The lines emitted when using SiO_2 and Al_2O_3 tubes were more persistent and they were observed in spectra up to 40 μs delay. In spectra obtained with the SiO_2 tube, two very narrow aluminum lines coming most probably from aluminum alloy ($AlMgCu_5$) electrodes were detected. Spectral lines from the electrode's material did not appear in BeO tube's spectra. The dust particles were formed in all three cases.

From the results of the spectroscopic studies with tubes made of different materials and at various plasma conditions, one can conclude that, if the space between the discharge tube and electrodes exists, a cooler discharge region is formed which enables the study of self-absorbed line shapes.

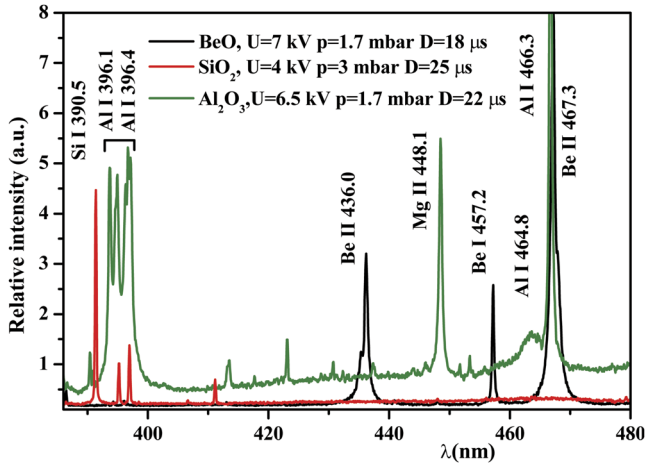

FIG. 7. Comparison of spectra from low pressure pulsed discharge observed for three different tubes under optimized conditions.

4. Plasma diagnostics

In order to characterize the plasma source, the electron density, N_e, and temperature, T_e, were determined by using the iterative method.

The electron number density during plasma afterglow was estimated using peak separation $\Delta\lambda_{ps}$ of the hydrogen Balmer beta line by using formula (6) from Ref. 32,

$$\log N_e\,(\mathrm{m}^{-3}) = A + B\,\log\,\Delta\lambda_{ps}(\mathrm{nm}) = 22.65 + 1.53\,\log\,\Delta\lambda_{ps}(\mathrm{nm}). \quad (1)$$

In order to use that formula, the value of T_e was presupposed to be 13 000 ± 3000 K, and based on T_e, the corresponding value of parameters A and B was taken from Ref. 32. Using this range of T_e, the uncertainty of N_e was 30%. For, in such a way, determined electron number densities, the temperature was estimated from the ratio of Be II 467.3 nm/Be I 457.3 using the following formula:

$$\frac{I_1}{I_2} = \frac{h^3}{2(2\pi mk)^{3/2}}\frac{(gA)_1\lambda_1 N_e}{(gA)_2\lambda_2 T_e^{3/2}}\exp\left(\frac{E_2 - E_1 + E_1^{ion} - \Delta E}{kT_e}\right), \quad (2)$$

where $E_1{}^{ion}$ is the ionization potential and ΔE is the ionization potential lowering.

After few iteration, N_e and T_e were determined. Transition probabilities were taken from the NIST database.[33]

Succeeding the determination of the excitation temperature and electron density, it is necessary to check if the conditions for LTE (Local Thermodynamic Equilibrium) have been met. The expression (12) from Ref. 34 in the case of beryllium sets the boundary value of the electron concentration to be 2.85×10^{22} m^{-3} for the temperature of 14 200 K. This means that the conditions for the complete LTE in the plasma used in this experiment have been met. Given that only three neutral and three ionic spectral lines were recorded, and considering that those transitions have very similar upper level energies, the use of the Boltzmann plot could not provide more precise values of N_e and T_e.

The temporal evolution of T_e and N_e during plasma afterglow is presented in Fig. 8.

It can be seen from Fig. 8 that N_e has increased after the end of the current pulse. The second maximum of N_e

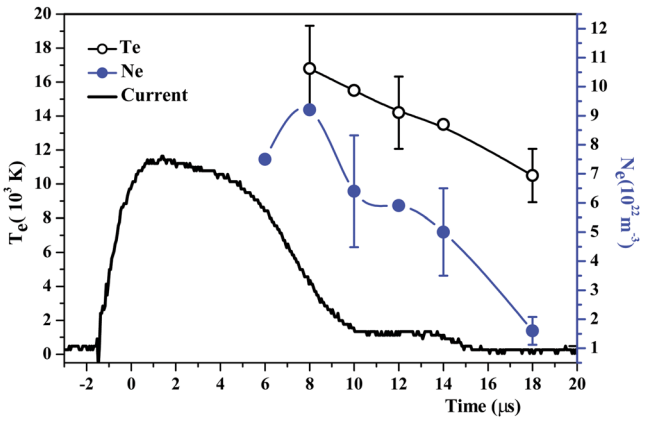

FIG. 8. Evolution of T_e and N_e. N_e is determined from peak separation of the hydrogen Balmer beta line,[32] and T_e is estimated using the ratio of intensities of beryllium lines, Be II 467.3 nm and Be I 457.3.

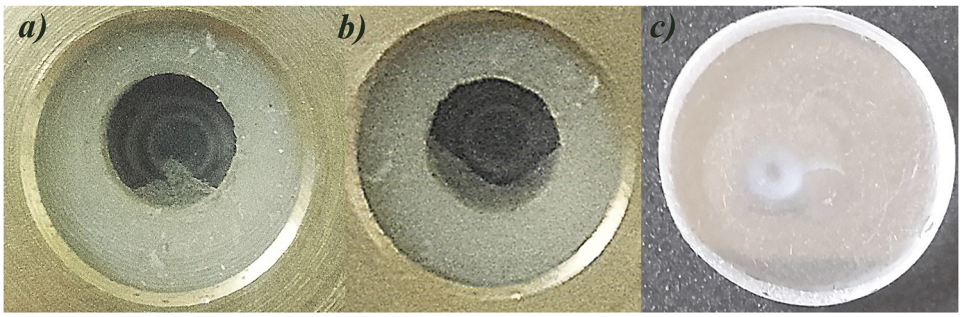

FIG. 9. Two forms of dust deposits: (a) cone, (b) half-moon, (c) degradation of the observation window caused by dust particles' deposition.

coincides with the second maximum of the current pulse, i.e., with the time position characterized by the most intense Be spectral lines around 12 μs. As a conclusion, it can be said that optimal conditions for Be spectral line shape measurements are achieved with C = 5 μF, U = 7 kV, gas Ar + 3% H_2, and p = 1.2 mbar and that Be lines reach their maximum intensity at t = 12 μs.

D. Generation of dust particles

Throughout the course of the source construction and optimization of Be line shape measurements, significant quantity of the dust was produced. The appearance of the dust particles may be related to the existence of the second current maximum which is most likely to be a consequence of the formation of negative ions that are the precursors of particle formation;[35] see Fig. 2. Namely, the electron density, as shown in Fig. 8, follows the current shape and this increase of the electron density after the main current pulse could be related to the charging and de-charging (ionization and recombination) of particles inside the plasma volume, as observed earlier in the pulsed complex plasma.[36,37] Anomalous behavior of the current pulse was used as a first sign that beryllium was ablated from the tube wall and that the Be spectral line should appear in the observed spectrum. Visible dust particles in the discharge were observed in the form of deposits on the observation window. These particles were noticed with gas flowing from the discharge tube support toward the output window. With the increase of discharge voltage, the generation of dust particles became more pronounced and appearance of the dust particles' deposit on the observation window became clearly visible. After a few operational hours, the deposit covered window completely decreasing optical signal to that extent that further spectroscopic measurements were impossible. The interesting fact is that with subsequent current pulses two forms of the dust deposits were observed: cone shaped after odd current pulse and "half ring" shaped after even current pulse; see Figs. 9(a) and 9(b), respectively, and the supplementary material in the form of movie. All measurements had to be taken in 1 h, and after this time the accumulated dust had to be removed and window had to be cleaned. To enable longer measurements, the gas flow direction was reversed, meaning gas was flowing from the output window toward the discharge tube support; see Sec. III C 1. In this configuration, dust deposits were not observed, but the degradation of window still occurred; see Fig. 9(c). This degradation of the window stopped occurring when the special inlet at an angle of 45° with respect to the discharge tube axis was installed; see Fig. 3(c). This inlet did not prevent the degradation of the window when working with pressures less than 1 mbar and voltages higher than 7 kV.

Deposits on the observation window were easily cleaned and since the BeO is highly toxic, the dust particles were collected by exfoliation using adhesive tape, with all safety precautions; see Sec. III A. After that, tape was folded in order to insure dust particle isolation. When larger quantities of dust was collected from the discharge tube or from the liquid nitrogen trap, a special handling and disposal procedure was performed. The dust particles were mixed with the PMMA component in the glass bowel, after that the second component, resin, was added and the polymer with BeO dust was produced. In such a way, safe handling and disposal of toxic dust was enabled. For further precaution, the glass bowel is closed with the lid, thus preventing the possibility of evaporation if heated.

In order to study conditions for producing dust particles in the discharge, two additional tubes made from alumina and quartz were constructed; see the description in Sec. III A. For both tubes, dust particles were formed. Indication for dust formation was the appearance of the second current maximum; see Fig. 2(b). Although the occurrence and duration of the second current maximum, hence dust production, were slightly different for all three tubes, there were some common features: the dust was always formed when Ar was used as discharge gas; smaller retention of particles was observed for higher pressures; the deposition of particles on the observation window was more pronounced when working with low pressures and high voltages. However, two forms of dust deposits (cone shaped and "half ring"), which can be seen when working with the BeO tube, were not noticed. Also, with the SiO_2 tube, dust was accumulated on the window even with reverse gas flow and with a 45° angle inlet installed.

The study about the influence of dust movements on spectral line shapes is in progress. Due to the high toxicity of dust, the shapes and dimensions of the obtained particles were not studied in this work.

IV. CONCLUSIONS

In this work, the construction details and optimization of the low pressure pulsed discharge for safe beryllium spectra studies in the presence and in the absence of dust particles were presented. Beryllium lines were obtained from erosion of the discharge tube made of beryllium oxide ceramic, BeO.

Electrical and spectroscopic studies were used for determination of the capacitance C, discharge voltage, gas type, and pressure, as well as electrodes distance, diameter of electrode openings, and other construction details. As a result, optimal conditions for beryllium lines observation are determined: low inductance 5 μF capacitor charged to 7 kV, 1.2 mbar of Ar + 3% H_2, 3 mm diameter of the electrode opening and the smallest possible distance between electrodes and ceramic tube, see Fig. 3 and Sec. III C 2. At discharge voltages greater than 7 kV, the productions of dust particles became excessive, thus preventing the study of the discharge tube material's particles on spectral line shapes. Using discharge tube modifications, i.e., with the gas inlet at 45° angle and reversed gas flow, longer measurements were enabled.

Under the optimized conditions, studies of Be lines in the presence of the Be dust were enabled for the first time. From the point of signal to noise ratio, optimal emission spectra of Be were obtained from 10 to 20 μs (measured from the beginning of the discharge), Fig. 2, coincident with the time of the second current maximum appearance. This shape of the current pulse was used as a first sign that beryllium was ablated from the tube wall and that the Be spectral line should appear in the observed spectrum. Stable operation of this novel beryllium plasma source creates the possibility of deepening the knowledge about the atomic data of Be, very much needed for the *in situ* examination of plasma facing materials in the tokamak by LIBS.

Hypothesis of relation between the second current maximum and optimal spectral emission from the tube material was proved using two additional tubes made of SiO_2 and Al_2O_3, even though discharge conditions differ. The dust particles were formed from all the three tubes. In this way, it is shown that this kind of low pressure pulsed discharge can be used for dust production and introduction of various materials into the plasma.

SUPPLEMENTARY MATERIAL

See supplementary material for the illustrations of two forms of dust deposits inside the discharge tube.

ACKNOWLEDGMENTS

This work has been financed by the Ministry of Education and Technological Development of the Republic of Serbia under the Project No. 171014. The authors thank Academician Professor Emeritus Nikola Konjević for correcting manuscript and Stanko Milanović for technical assistance in preparation and setting up the experiment.

[1] G. Gilmore, B. Gustafsson, B. Edvardsson, and P. E. Nissen, Nature **357**, 379 (1992).
[2] M. C. Galvez-Ortiz, E. Delgado-Mena, J. I. Gonzalez Hernandez, G. Israelian, N. C. Santos, R. Rebolo, and A. Ecuvillon, Astron. Astrophys. **530**, A66 (2011).
[3] N. Konjević and J. R. Roberts, J. Phys. Chem. Ref. Data **5**, 209 (1976).
[4] N. Konjević and W. L. Wiese, J. Phys. Chem. Ref. Data **5**, 259 (1976).
[5] N. Konjević, M. S. Dimitrijević, and W. L. Wiese, J. Phys. Chem. Ref. Data **13**, 619 (1984).
[6] N. Konjević, M. S. Dimitrijević, and W. L. Wiese, J. Phys. Chem. Ref. Data **13**, 649 (1984).
[7] N. Konjević and W. L. Wiese, J. Phys. Chem. Ref. Data **19**, 1307 (1990).
[8] N. Konjević, A. Lesage, J. R. Fuhr, and W. L. Wiese, J. Phys. Chem. Ref. Data **31**, 819 (2002).
[9] A. Lesage, New Astron. Rev. **52**, 471 (2009).
[10] M. Platiša, J. Purić, N. Konjević, and J. Labat, Astron. Astrophys. **15**, 325 (1971), available at http://adsabs.harvard.edu/abs/1971A%26A....15..325P.
[11] J. Purić and N. Konjević, Z. Phys. **249**, 440 (1972).
[12] D. Hadžiomerspahić, M. Platiša, N. Konjević, and M. Popović, Z. Phys. **262**, 169 (1973).
[13] A. Sanchez, M. Blaha, and W. W. Jones, Phys. Rev. A **8**, 774 (1973).
[14] H. P. Klug, Rev. Sci. Instrum. **12**, 155 (1941).
[15] H. Brackney and Z. J. Atlee, Rev. Sci. Instrum. **14**, 59 (1943).
[16] International Thermonuclear Fusion Experimental Reactor Project, ITER Report, ITER D 2X6K67 v1.0 Plant Description (PD), Cadarache, 2009.
[17] T. J. Dolan, *Magnetic Fusion Technology* (Springer, London, 2013).
[18] I. B. Kupriyanov, G. N. Nikolaev, L. A. Kurbatova, N. P. Porezanov, V. L. Podkovyrov, A. D. Muzichenko, A. M. Zhitlukhin, A. A. Gervash, and V. M. Safronov, J. Nucl. Mater. **463**, 781 (2015).
[19] G. R. Longhurst, L. L. Snead, and A. A. Abou-Sena, in *Proceedings of the Sixth International Workshop on Beryllium Technology for Fusion (Miyazaki, Japan)* (JAERI, 2004), Vol. 36, p. 2, available at 10.11484/conf/JAERI-Conf-2004-006.pdf.
[20] Z. Wang and C. M. Ticos, Rev. Sci. Instrum. **79**, 10F333 (2008).
[21] U. Kortshagen, J. Phys. D: Appl. Phys. **45**, 253001 (2012).
[22] P. K. Shukla and B. Eliasson, Rev. Mod. Phys. **81**, 25 (2009).
[23] G. E. Morfill and A. V. Ivlev, Rev. Mod. Phys. **81**, 1353 (2009).
[24] A. Piel and A. Melzer, Plasma Phys. Controlled Fusion **44**, R1 (2002).
[25] N. H. Brooks, A. Howald, K. Klepper, and P. West, Rev. Sci. Instrum. **63**, 5167 (1992).
[26] R. J. Colchin, D. L. Hillis, R. Maingi, C. C. Klepper, and N. H. Brooks, Rev. Sci. Instrum. **74**, 2068 (2003).
[27] V. Morel, B. Pérès, A. Bultel, A. Hideur, and C. Grisolia, Phys. Scr. **T167**, 014016 (2016).
[28] A. Semerok, D. L'Hermite, J. M. Weulersse, J. L. Lacour, G. Cheymol, M. Kempenaars, N. Bekris, and C. Grisolia, Spectrochim. Acta, Part B **123**, 121 (2016).
[29] See https://www-s.nist.gov/srmors/msds/1877-MSDS.pdf for toxicological information, see Sect. 11.
[30] M. Ivković, T. Gajo, I. Savić, and N. Konjević, J. Quant. Spectrosc. Radiat. Transfer **161**, 197 (2015).
[31] T. Gajo, M. Ivković, N. Konjević, I. Savić, S. Djurović, Z. Mijatović, and R. Kobilarov, Mon. Not. R. Astron. Soc. **455**, 2969 (2016).
[32] M. Ivković, N. Konjević, and Z. Pavlović, J. Quant. Spectrosc. Radiat. Transfer **154**, 1 (2015).
[33] J. R. Fuhr and W. L. Wiese, J. Phys. Chem. Ref. Data **39**, 013101 (2010).
[34] H. R. Griem, Phys. Rev. **131**, 1170 (1963).
[35] L. Boufendi, J. Hermann, A. Bouchoule, B. Dubreuil, E. Stoffels, W. W. Stoffels, and M. L. de Giorgi, J. Appl. Phys. **76**, 148 (1994).
[36] J. Berndt, E. Kovačević, V. Selenin, I. Stefanović, and J. Winter, Plasma Sources Sci. Technol. **15**, 18 (2006).
[37] I. Stefanović, N. Sadeghi, J. Winter, and B. Sikimić, Plasma Sources Sci. Technol. **26**, 065014 (2017).